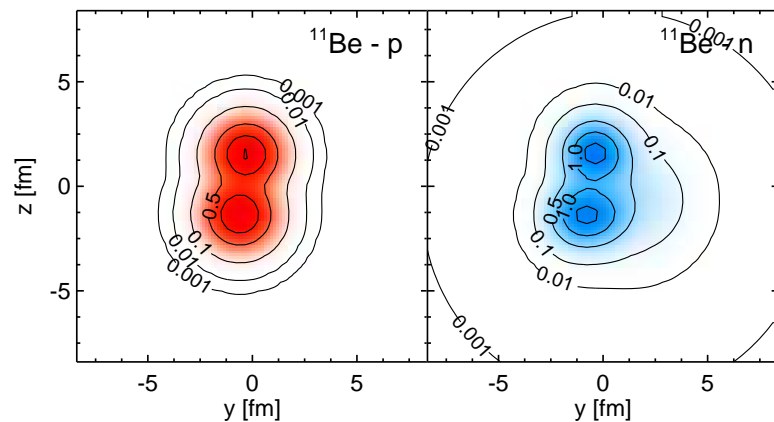


Beryllium Isotopes studied in Fermionic Molecular Dynamics



Thomas Neff

2nd EMMI-EFES Workshop on
Neutron-Rich Exotic Nuclei
EENEN10

RIKEN, Tokyo
June 16, 2010

Overview



Effective Nucleon-Nucleon interaction:

Unitary Correlation Operator Method

Roth, Neff, Feldmeier, Prog. Part. Nucl. Phys. 65 (2010) 50

- **Short-range Central and Tensor Correlations**
- ***ab initio* Few-Body Calculations**

Many-Body Method:

Fermionic Molecular Dynamics

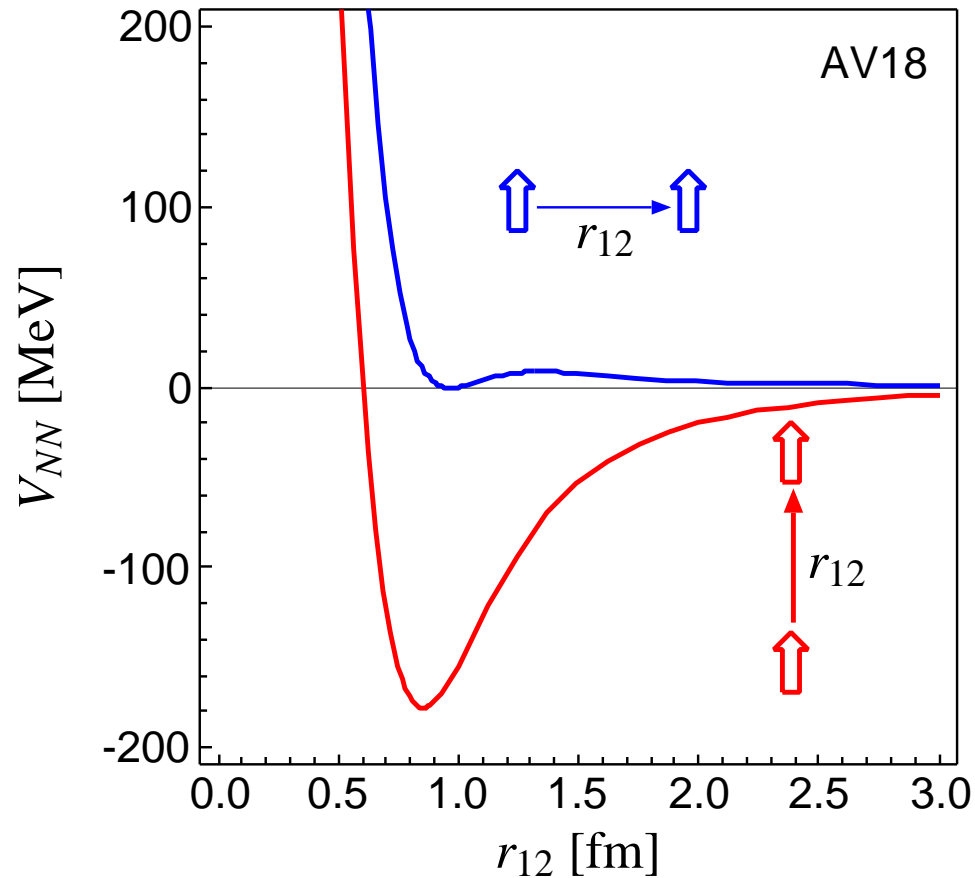
- **Model**
- **Beryllium Isotopes**

Unitary Correlation Operator Method

Nuclear Force

Argonne V18 (T=0)

spins aligned parallel or perpendicular to the relative distance vector



- strong repulsive core: nucleons can not get closer than ≈ 0.5 fm

➤ **central correlations**

- strong dependence on the orientation of the spins due to the tensor force

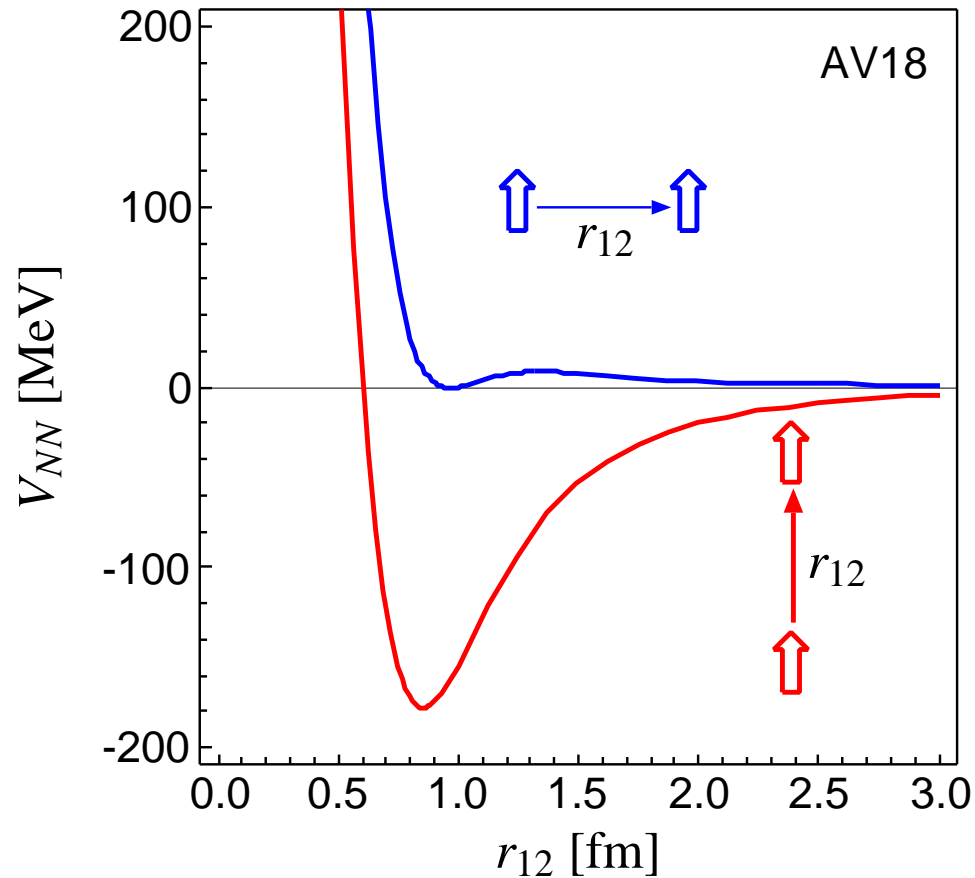
➤ **tensor correlations**

Unitary Correlation Operator Method

Nuclear Force

Argonne V18 (T=0)

spins aligned parallel or perpendicular to the relative distance vector



- strong repulsive core: nucleons can not get closer than ≈ 0.5 fm

➤ **central correlations**

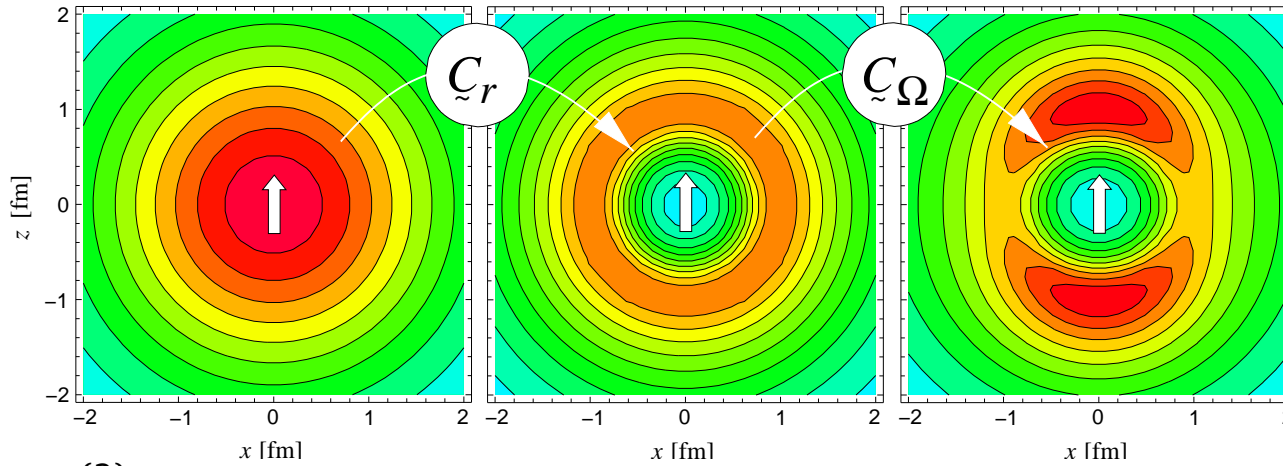
- strong dependence on the orientation of the spins due to the tensor force

➤ **tensor correlations**

the nuclear force will induce **strong short-range correlations** in the nuclear wave function

- Unitary Correlation Operator Method
- Realistic Effective Interaction

two-body densities



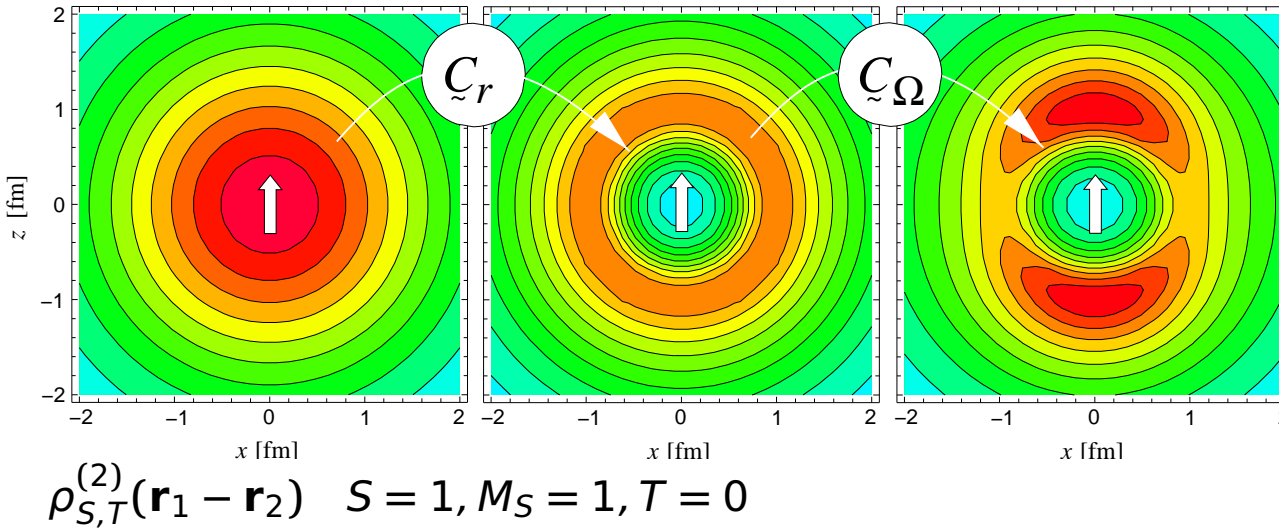
$$\rho_{S,T}^{(2)}(\mathbf{r}_1 - \mathbf{r}_2) \quad S = 1, M_S = 1, T = 0$$

central correlator \tilde{C}_r
shifts density out of
the repulsive core

tensor correlator \tilde{C}_Ω
aligns density with spin
orientation

Unitary Correlation Operator Method Realistic Effective Interaction

two-body densities

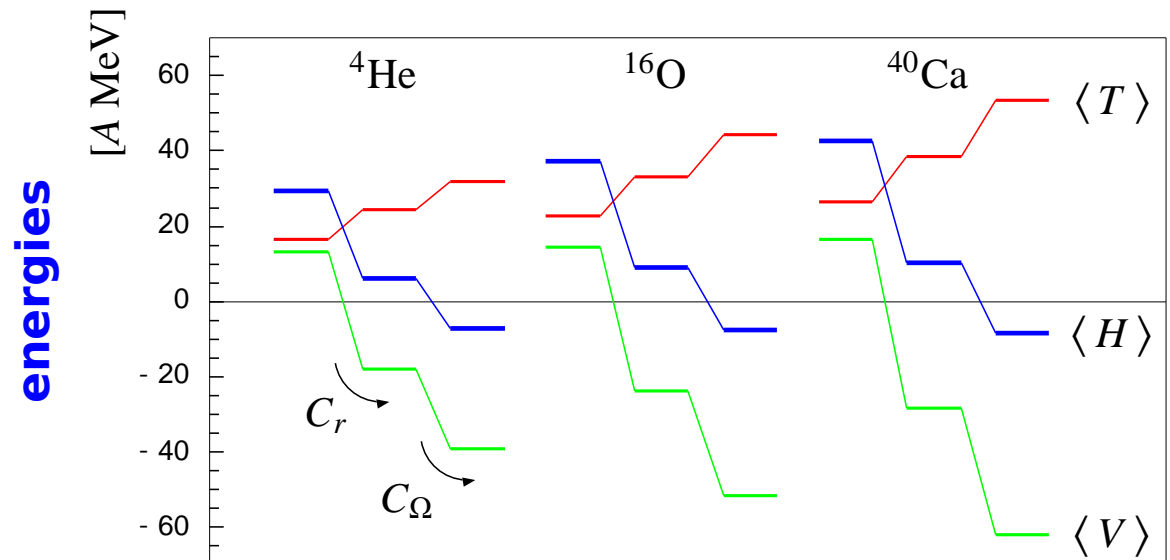


central correlator \tilde{C}_r
shifts density out of
the repulsive core

tensor correlator \tilde{C}_Ω
aligns density with spin
orientation

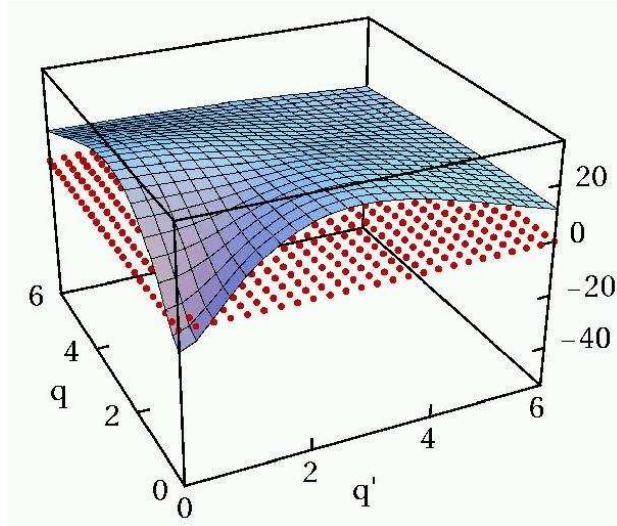
both central
and tensor
correlations are
essential for
binding

$0\hbar\omega$ Harmonic Oscillator



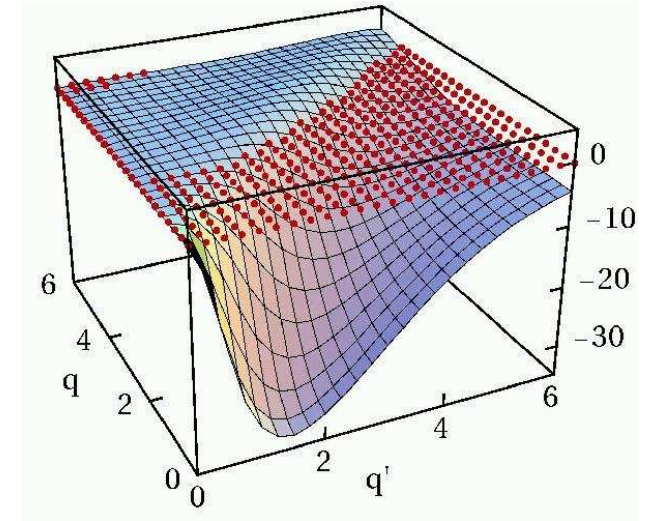
- Unitary Correlation Operator Method
- **Correlated Interaction in Momentum Space**

3S_1 bare



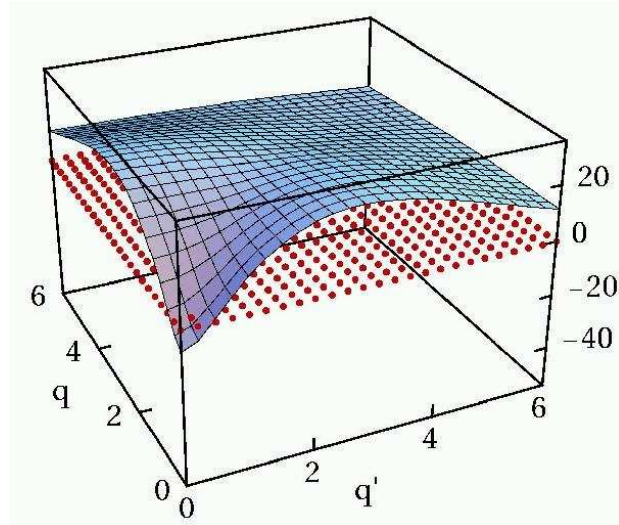
bare interaction has **strong off-diagonal** matrix elements connecting to high momenta

${}^3S_1 - {}^3D_1$ bare



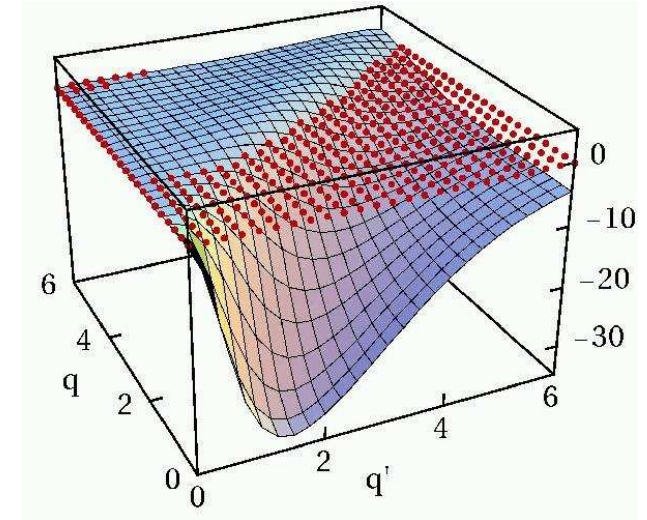
- Unitary Correlation Operator Method
- **Correlated Interaction in Momentum Space**

3S_1 bare



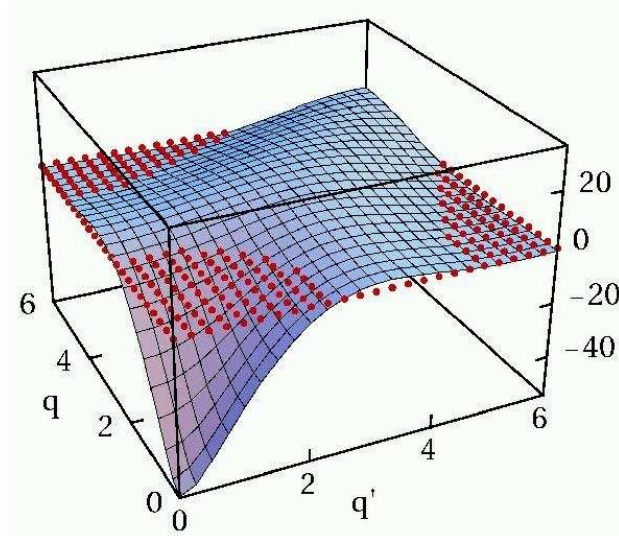
bare interaction has **strong off-diagonal** matrix elements connecting to high momenta

${}^3S_1 - {}^3D_1$ bare



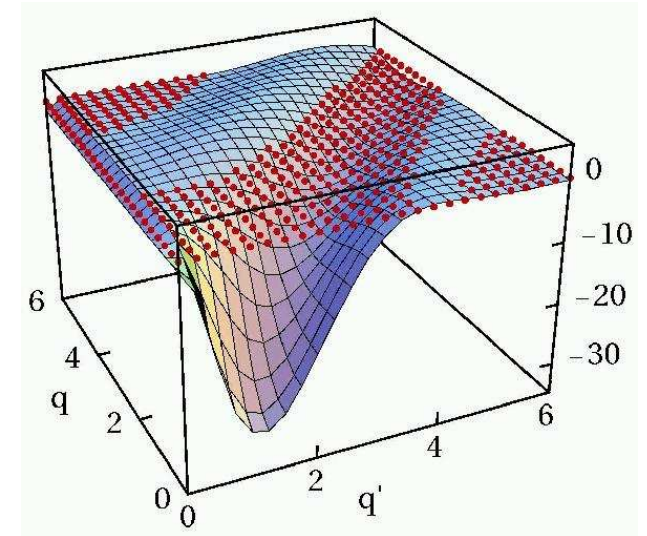
correlated interaction is **more attractive** at low momenta

3S_1 correlated



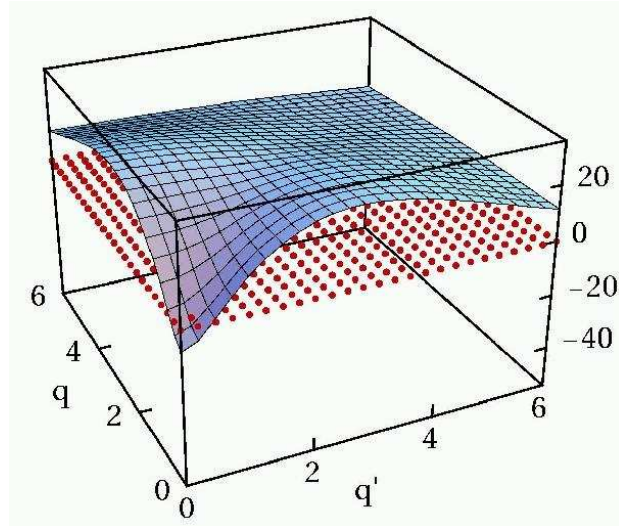
off-diagonal matrix elements connecting low- and high- momentum states are **strongly reduced**

${}^3S_1 - {}^3D_1$ correlated



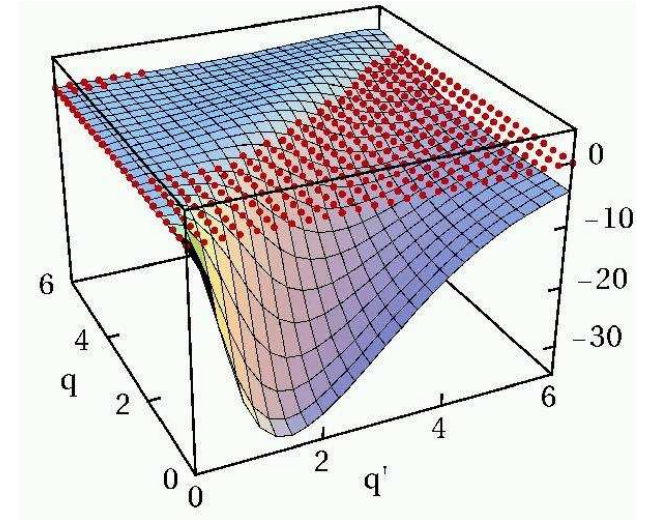
- Unitary Correlation Operator Method
- **Correlated Interaction in Momentum Space**

3S_1 bare



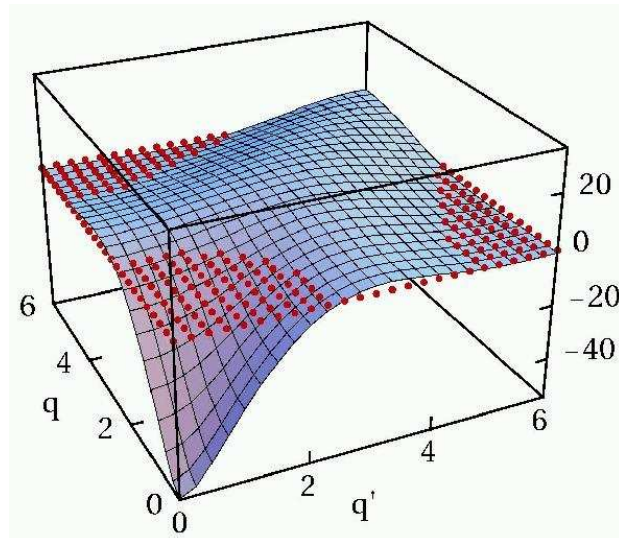
bare interaction has **strong off-diagonal** matrix elements connecting to high momenta

${}^3S_1 - {}^3D_1$ bare



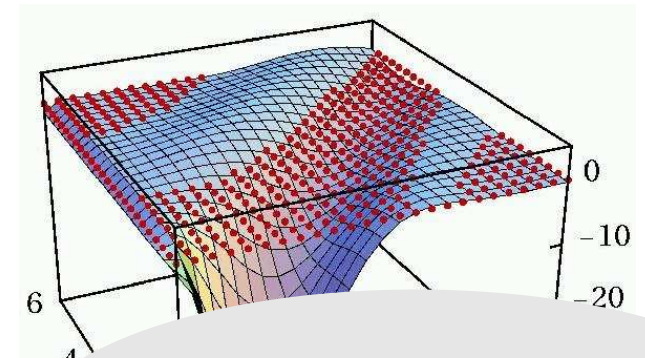
correlated interaction is **more attractive** at low momenta

3S_1 correlated



off-diagonal matrix elements connecting low- and high- momentum states are **strongly reduced**

${}^3S_1 - {}^3D_1$ correlated



similar to V_{low-k}
Bogner, Kuo, Schwenk,
Phys. Rep. **386**, 1 (2003)

Fermionic Molecular Dynamics



Motivation

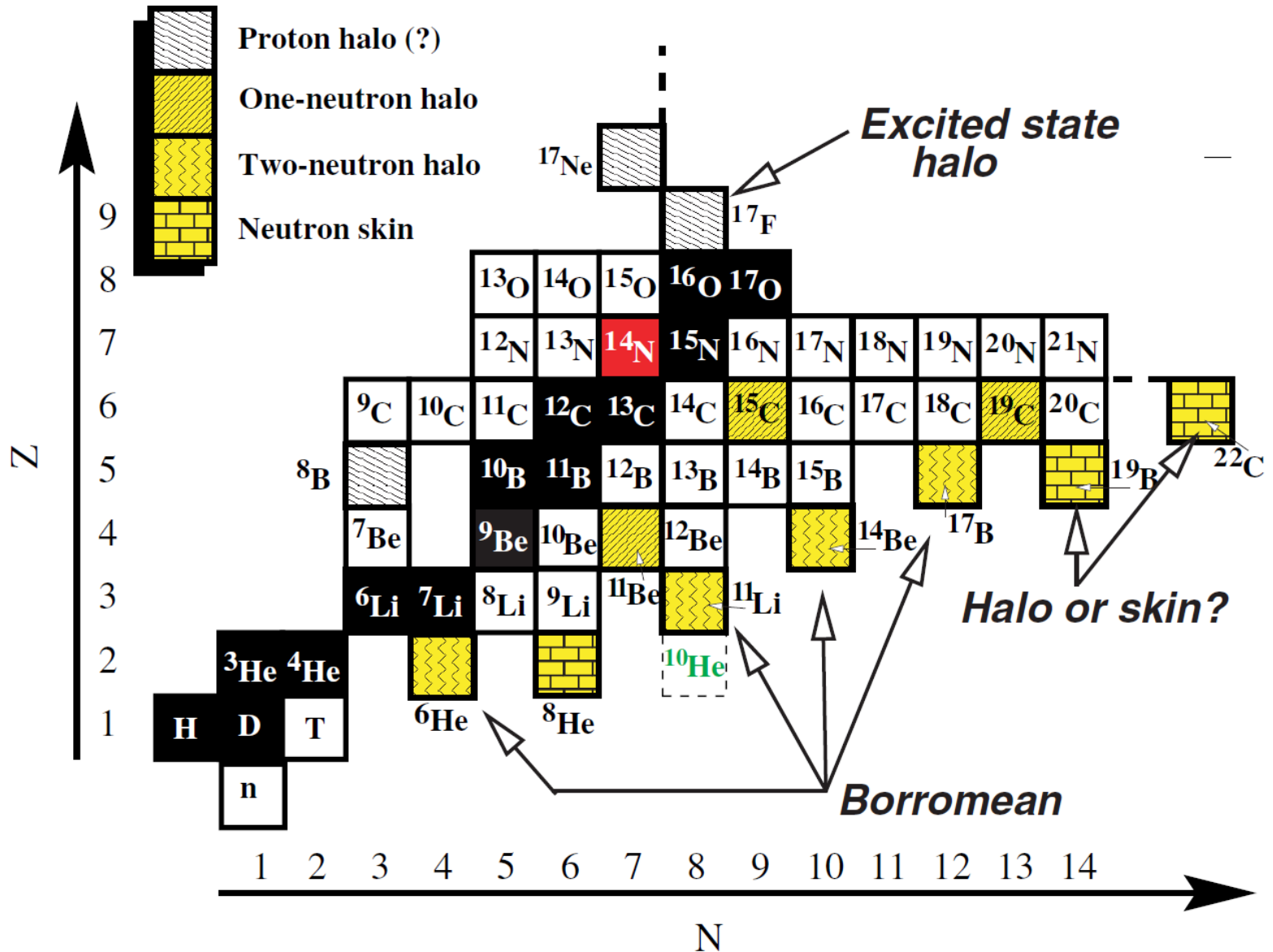
FMD Wave Functions

Nucleon-Nucleon Interaction

Mean-Field Calculations

**Projection After Variation,
Variation After Projection
and Multiconfiguration**

Exotica: Special Challenges



Fermionic

Slater determinant

$$|Q\rangle = \mathcal{A}\left(|q_1\rangle \otimes \cdots \otimes |q_A\rangle\right)$$

- antisymmetrized A -body state

Fermionic

Slater determinant

$$|Q\rangle = \mathcal{A}\left(|q_1\rangle \otimes \cdots \otimes |q_A\rangle\right)$$

- antisymmetrized A -body state

Molecular

single-particle states

$$\langle \mathbf{x} | q \rangle = \sum_i c_i \exp\left\{-\frac{(\mathbf{x} - \mathbf{b}_i)^2}{2a_i}\right\} \otimes |\chi_i^\uparrow, \chi_i^\downarrow\rangle \otimes |\xi\rangle$$

- Gaussian wave-packets in phase-space (complex parameter \mathbf{b}_i encodes mean position and mean momentum), spin is free, isospin is fixed
- width a_i is an independent variational parameter for each wave packet
- use one or two wave packets for each single particle state

Fermionic

Slater determinant

$$|Q\rangle = \mathcal{A}\left(|q_1\rangle \otimes \cdots \otimes |q_A\rangle\right)$$

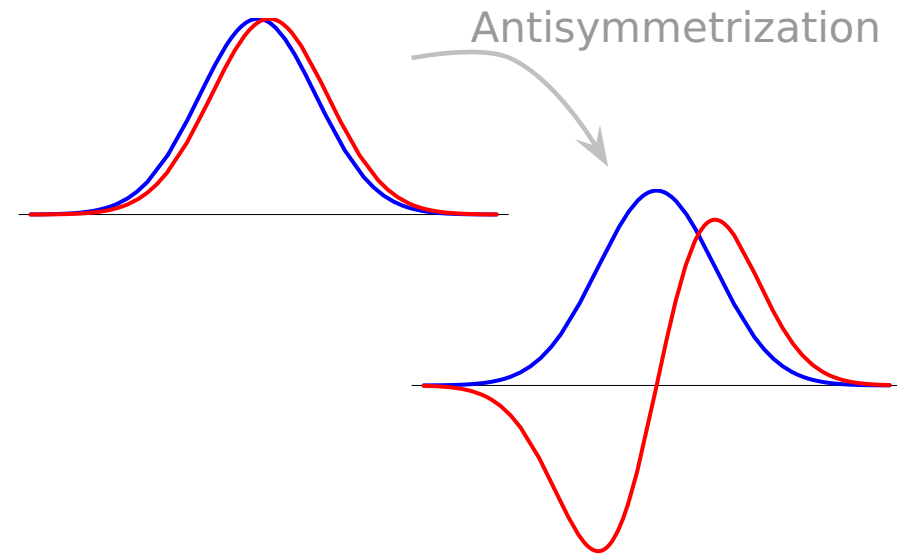
- antisymmetrized A -body state

Molecular

single-particle states

$$\langle \mathbf{x} | q \rangle = \sum_i c_i \exp\left\{-\frac{(\mathbf{x} - \mathbf{b}_i)^2}{2a_i}\right\} \otimes |\chi_i^\uparrow, \chi_i^\downarrow\rangle \otimes |\xi\rangle$$

- Gaussian wave-packets in phase-space (complex parameter \mathbf{b}_i encodes mean position and mean momentum), spin is free, isospin is fixed
- width a_i is an independent variational parameter for each wave packet
- use one or two wave packets for each single particle state



Fermionic

Slater determinant

$$|Q\rangle = \mathcal{A}\left(|q_1\rangle \otimes \cdots \otimes |q_A\rangle\right)$$

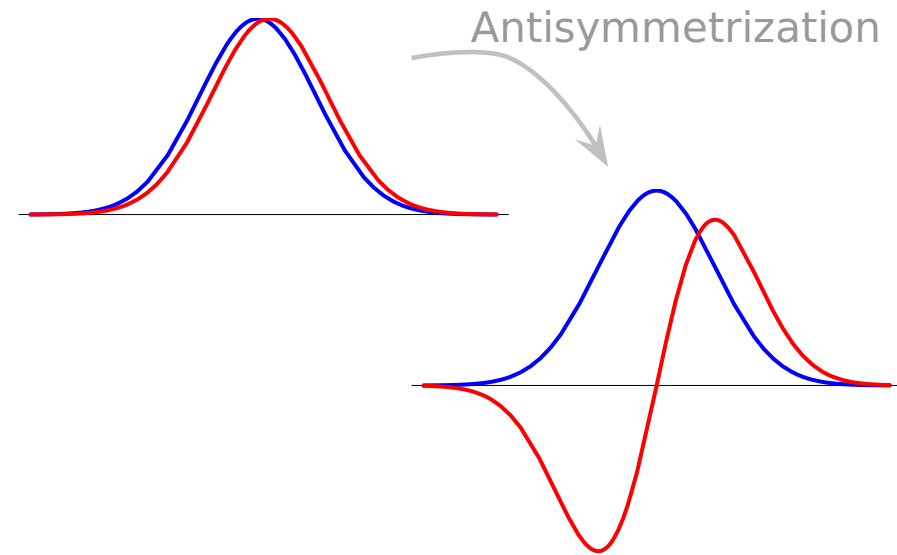
- antisymmetrized A -body state

Molecular

single-particle states

$$\langle \mathbf{x} | q \rangle = \sum_i c_i \exp\left\{-\frac{(\mathbf{x} - \mathbf{b}_i)^2}{2a_i}\right\} \otimes |\chi_i^\uparrow, \chi_i^\downarrow\rangle \otimes |\xi\rangle$$

- Gaussian wave-packets in phase-space (complex parameter \mathbf{b}_i encodes mean position and mean momentum), spin is free, isospin is fixed
- width a_i is an independent variational parameter for each wave packet
- use one or two wave packets for each single particle state



see also
**Antisymmetrized
 Molecular Dynamics**

H. Horiuchi, Y. Kanada-En'yo

Effective two-body interaction

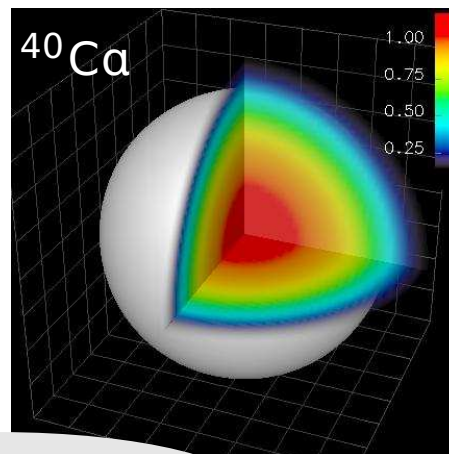
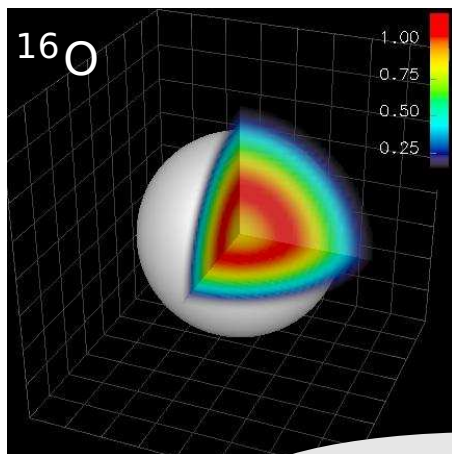
- FMD model space can't describe correlations induced by residual medium-long ranged tensor forces
- use **long ranged tensor correlator – “low cutoff”** to partly account for that
- no three-body forces: missing spin-orbit strength, saturation properties
- add phenomenological two-body correction term with a **momentum-dependent** central and (isospin-dependent) **spin-orbit** part (about 15% contribution to potential)
- fit correction term to binding energies and radii of “closed-shell” nuclei (^4He , ^{16}O , ^{40}Ca), (^{24}O , ^{34}Si , ^{48}Ca)
- **Outlook:**
use **three-body** or **density dependent two-body force** instead of two-body correction term

Minimization

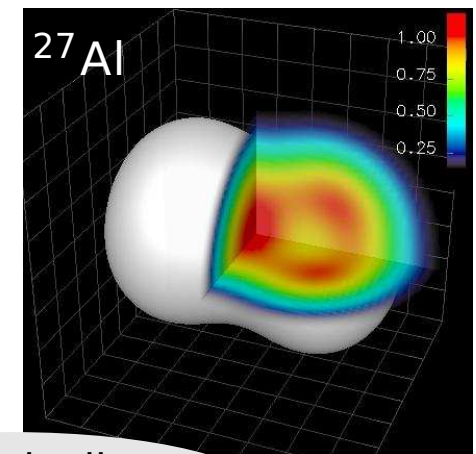
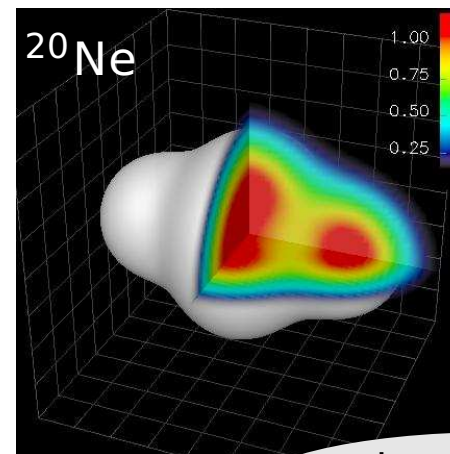
- minimize Hamiltonian expectation value with respect to all single-particle parameters q_k

$$\min_{\{q_k\}} \frac{\langle Q | \tilde{H} - \tilde{T}_{cm} | Q \rangle}{\langle Q | Q \rangle}$$

- this is a Hartree-Fock calculation in our particular single-particle basis
- the mean-field may break the symmetries of the Hamiltonian



spherical nuclei



intrinsically deformed nuclei

Projection After Variation (PAV)

- mean-field may break symmetries of Hamiltonian
- restore inversion, translational and rotational symmetry by projection on parity, linear and angular momentum

$$\tilde{P}^{\pi} = \frac{1}{2}(1 + \pi\Pi)$$

$$\tilde{P}_{MK}^J = \frac{2J+1}{8\pi^2} \int d^3\Omega D_{MK}^{J*}(\Omega) R(\Omega)$$

$$\tilde{P}^{\mathbf{P}} = \frac{1}{(2\pi)^3} \int d^3\mathbf{X} \exp\{-i(\tilde{\mathbf{P}} - \mathbf{P}) \cdot \mathbf{X}\}$$

Projection After Variation (PAV)

- mean-field may break symmetries of Hamiltonian
- restore inversion, translational and rotational symmetry by projection on parity, linear and angular momentum

$$\tilde{P}^\pi = \frac{1}{2}(1 + \pi\Pi)$$

$$\tilde{P}_{MK}^J = \frac{2J+1}{8\pi^2} \int d^3\Omega D_{MK}^{J*}(\Omega) \tilde{R}(\Omega)$$

Variation After Projection (VAP)

- effect of projection can be large
- full Variation after Angular Momentum and Parity Projection (VAP) for light nuclei
- perform VAP in GCM sense by applying **constraints** on **radius**, **dipole moment**, **quadrupole moment** or **octupole moment** and minimizing the energy in the projected energy surface for heavier nuclei

$$\tilde{P}^{\mathbf{P}} = \frac{1}{(2\pi)^3} \int d^3\mathbf{X} \exp\{-i(\tilde{\mathbf{P}} - \mathbf{P}) \cdot \mathbf{X}\}$$

PAV, VAP and Multiconfiguration

Projection After Variation (PAV)

- mean-field may break symmetries of Hamiltonian
- restore inversion, translational and rotational symmetry by projection on parity, linear and angular momentum

$$\tilde{P}^\pi = \frac{1}{2}(1 + \pi\Pi)$$

$$\tilde{P}_{MK}^J = \frac{2J+1}{8\pi^2} \int d^3\Omega D_{MK}^{J*}(\Omega) \tilde{P}(\Omega)$$

Variation After Projection (VAP)

- effect of projection can be large
- full Variation after Angular Momentum and Parity Projection (VAP) for light nuclei
- perform VAP in GCM sense by applying **constraints** on **radius**, **dipole moment**, **quadrupole moment** or **octupole moment** and minimizing the energy in the projected energy surface for heavier nuclei

$$\tilde{P}^{\mathbf{P}} = \frac{1}{(2\pi)^3} \int d^3\mathbf{X} \exp\{-i(\tilde{\mathbf{P}} - \mathbf{P}) \cdot \mathbf{X}\}$$

Multiconfiguration Calculations

- **diagonalize** Hamiltonian in a set of projected intrinsic states

$$\left\{ |Q^{(a)}\rangle, \quad a = 1, \dots, N \right\}$$

$$\sum_{K'b} \langle Q^{(a)} | \tilde{H} \tilde{P}_{KK'}^{J\pi} \tilde{P}^{\mathbf{P}=0} | Q^{(b)} \rangle \cdot c_{K'b}^\alpha = E^{J\pi\alpha} \sum_{K'b} \langle Q^{(a)} | \tilde{P}_{KK'}^{J\pi} \tilde{P}^{\mathbf{P}=0} | Q^{(b)} \rangle \cdot c_{K'b}^\alpha$$

Beryllium Isotopes



Questions

- α -clustering, halos in ^{11}Be and ^{14}Be , $N = 8$ shell closure ?

Calculation

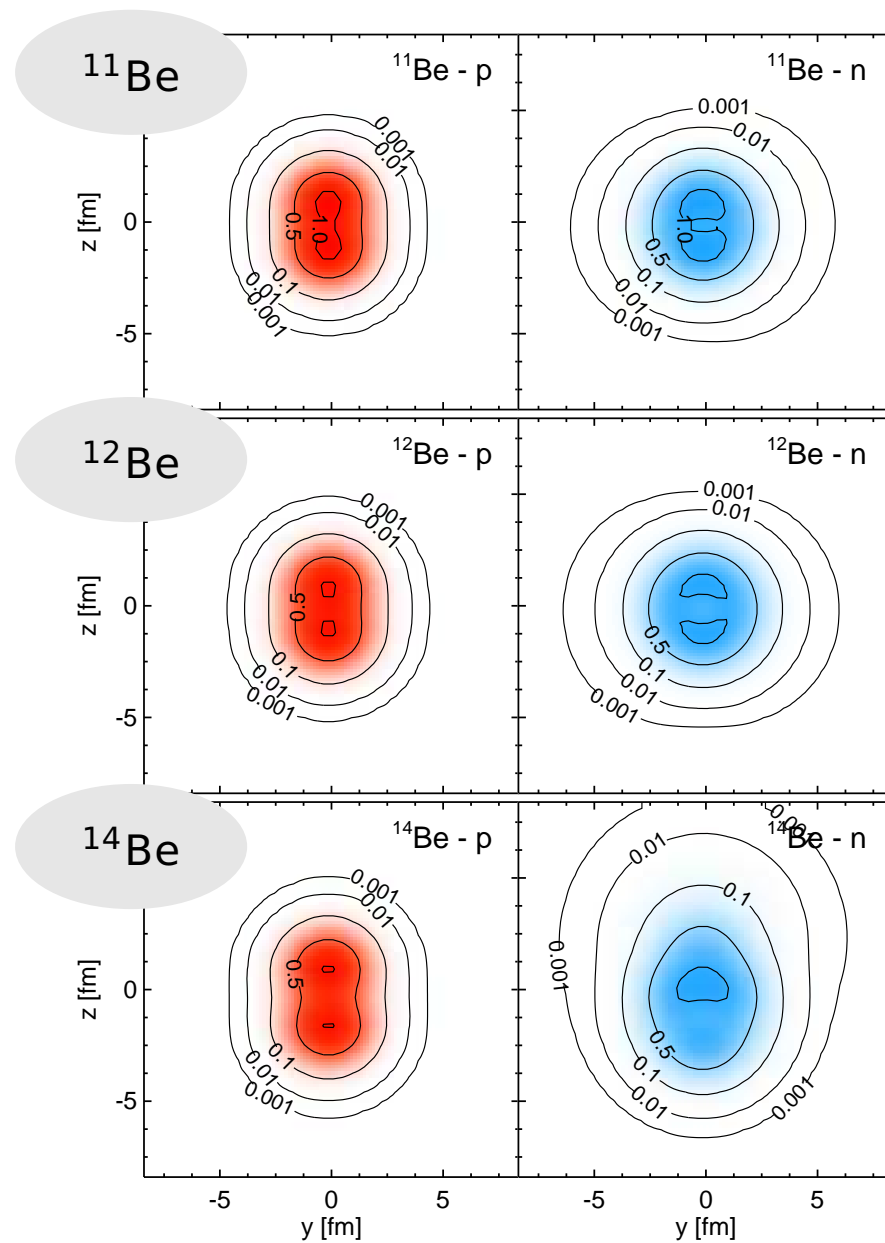
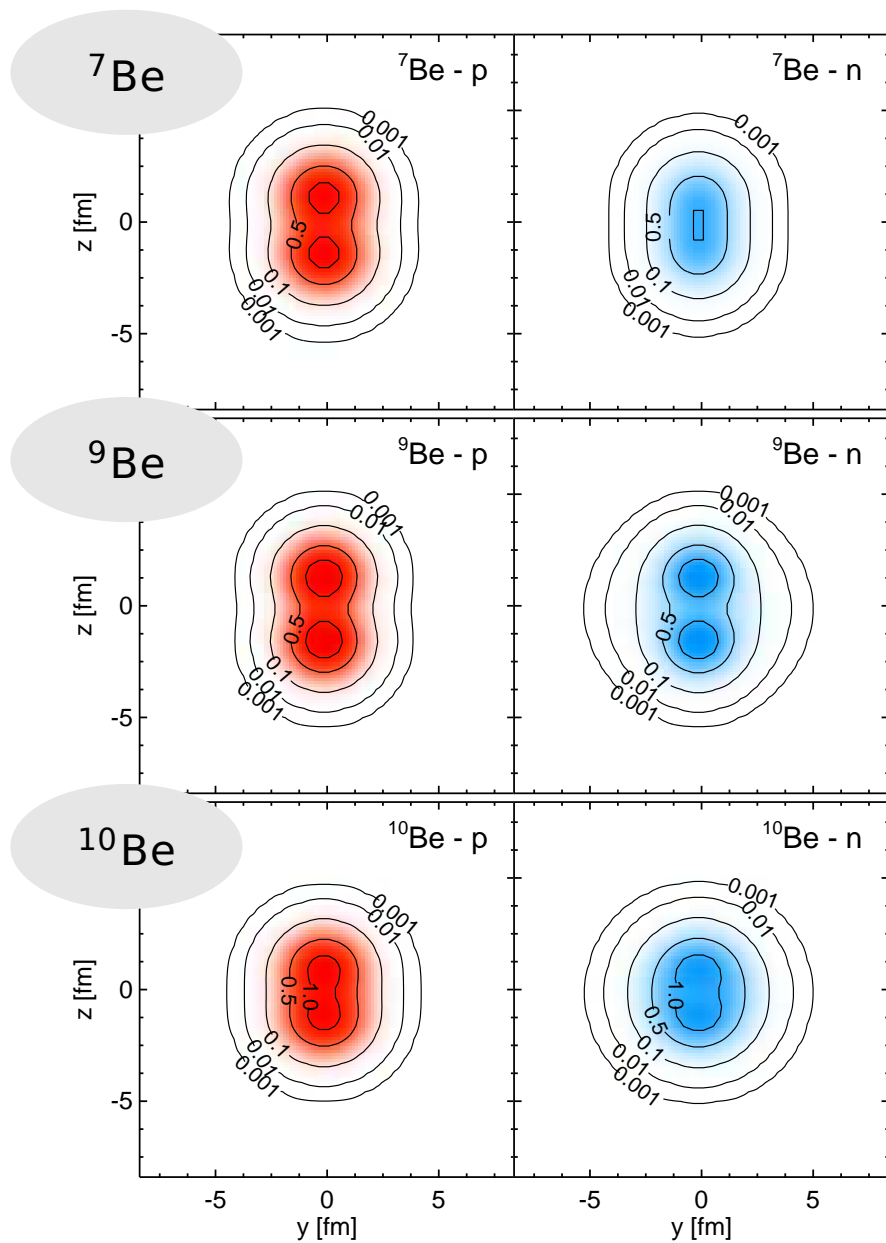
- FMD wave functions with two Gaussians per sp-state
- mean field, variation after projection, variation after multiconfiguration mixing
- VAP and multiconfiguration-VAP configurations with mean proton distance as generator coordinate

Observables

- energies
- charge and matter radii, electromagnetic transitions

Beryllium Isotopes

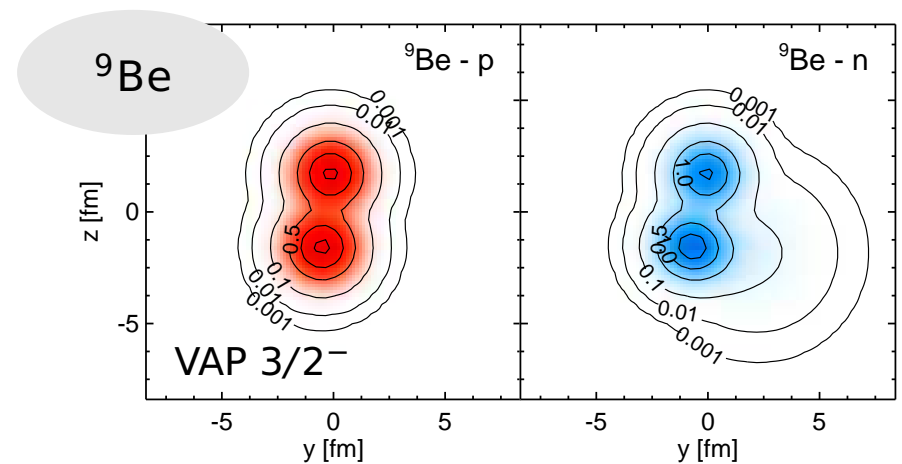
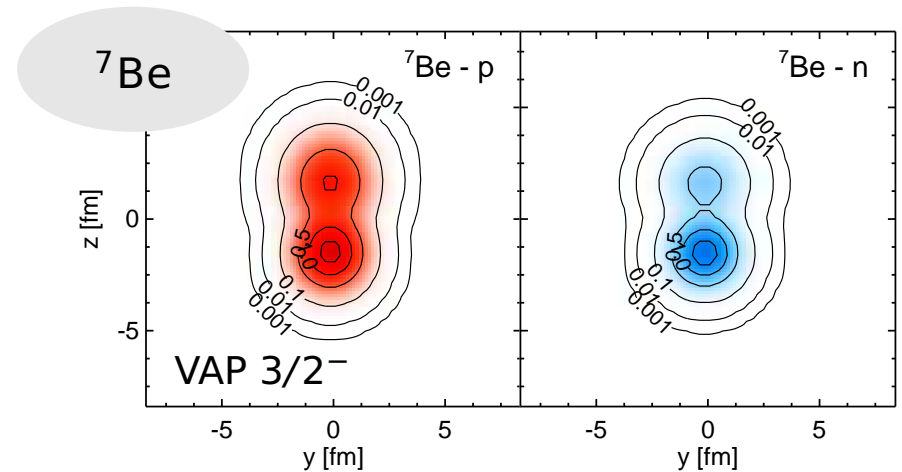
Mean field



Beryllium Isotopes

Variation after Projection

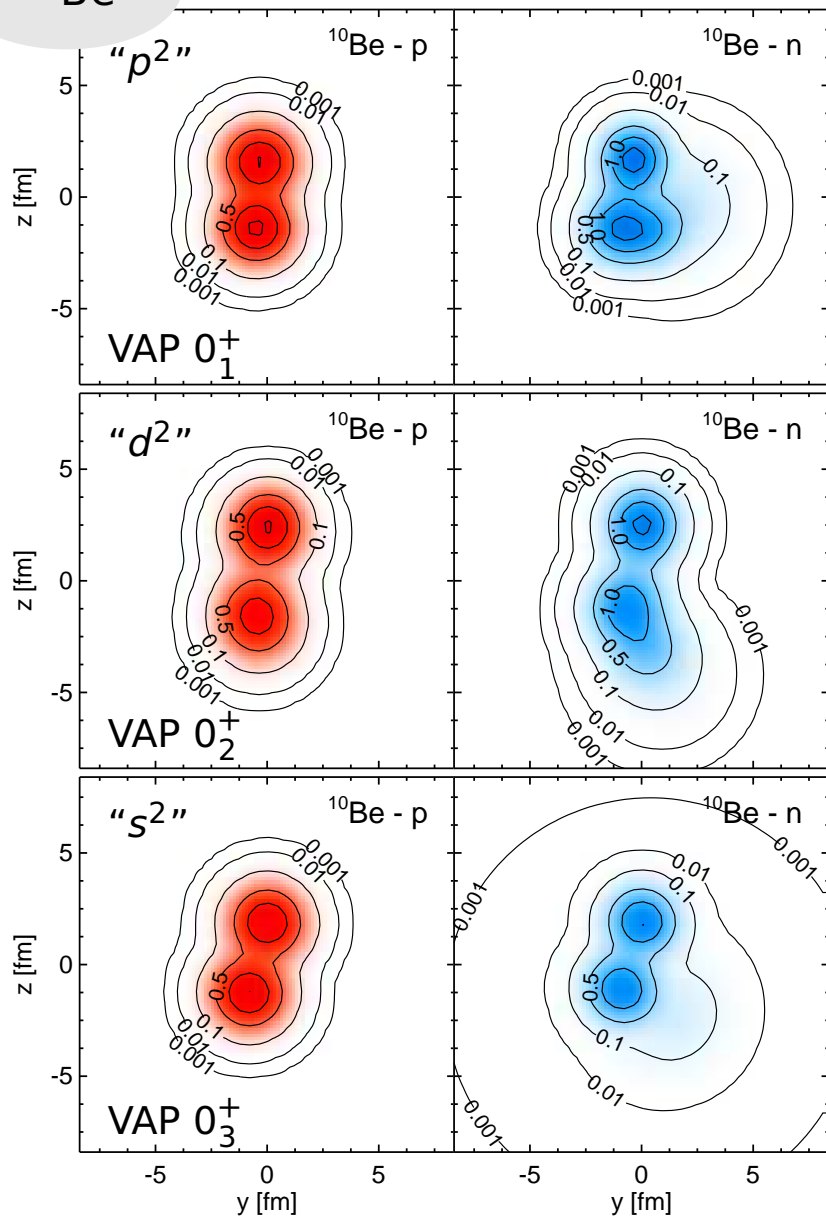
- create configurations by variation after parity and angular momentum projection
- large gain in binding energy compared to mean-field result
- intrinsic states show pronounced cluster structure. Parameters of ^4He and ^3He clusters are close to those of the free clusters



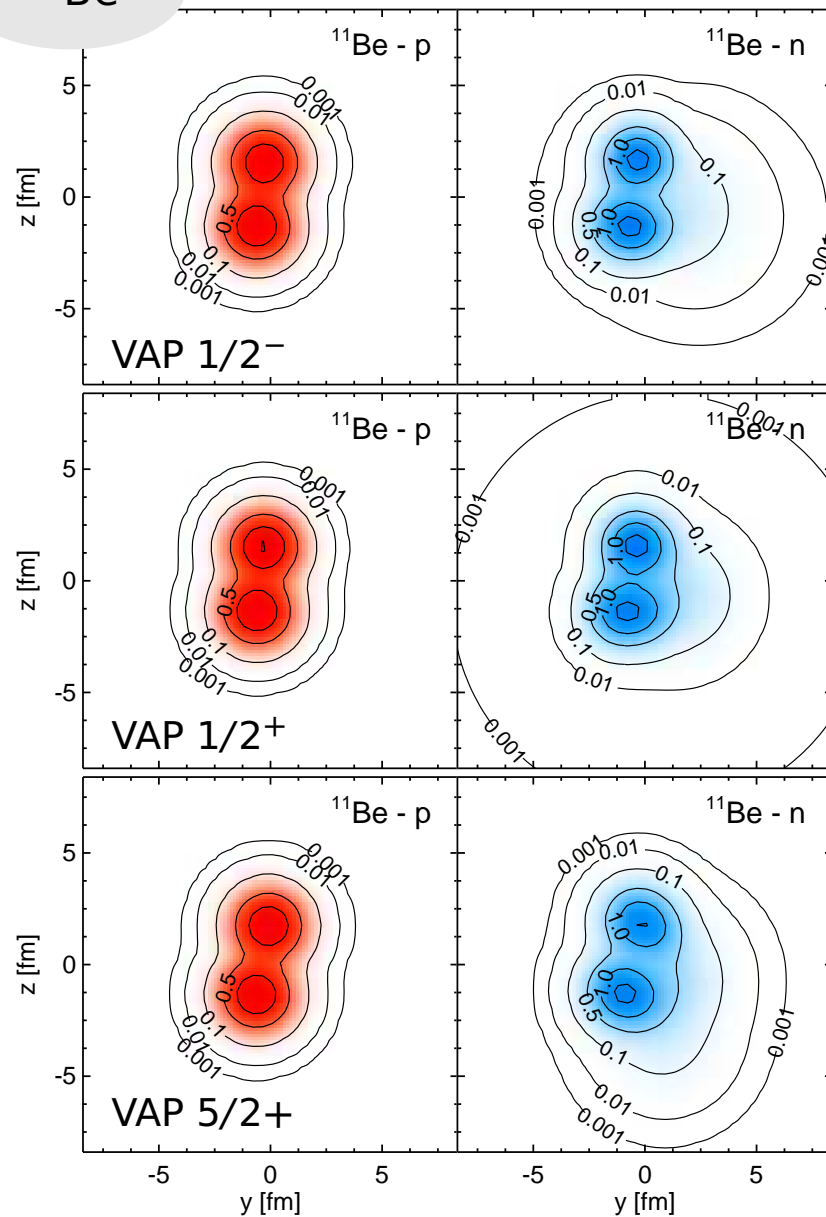
Beryllium Isotopes

Variation after Projection

^{10}Be



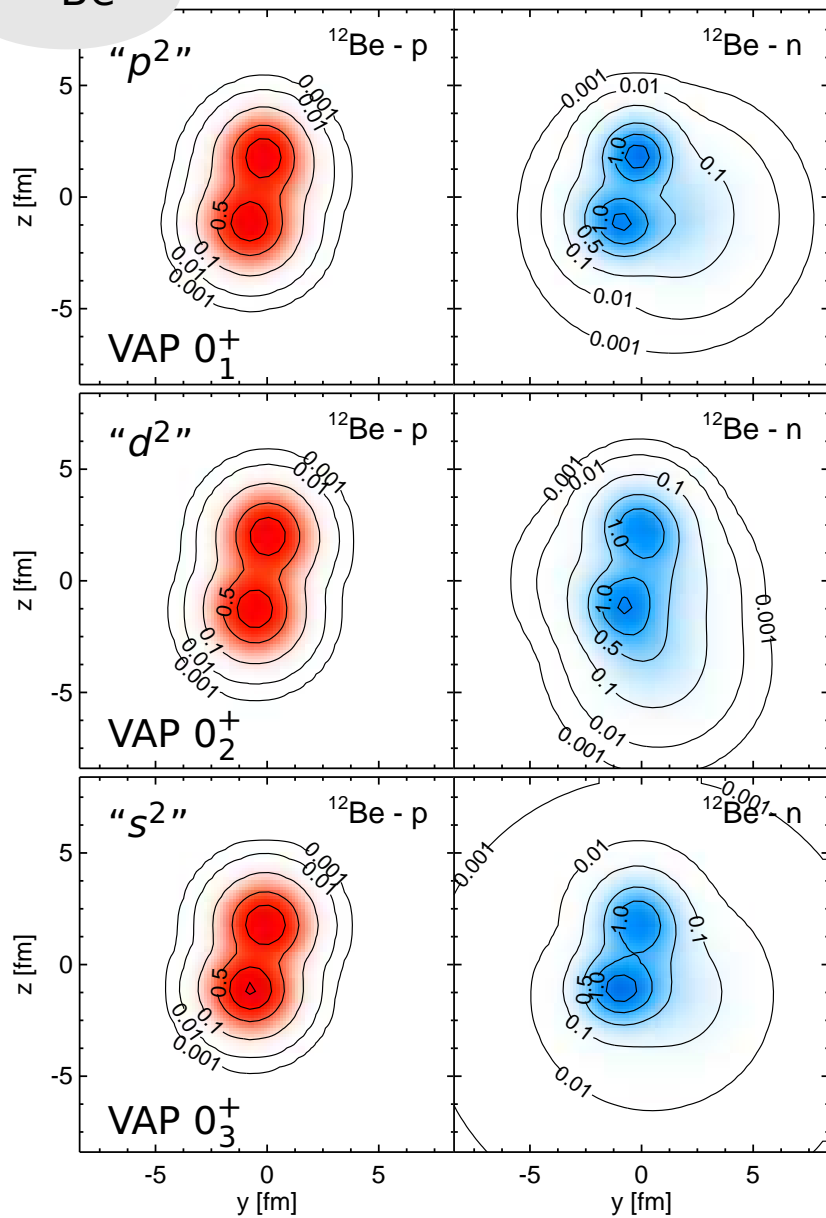
^{11}Be



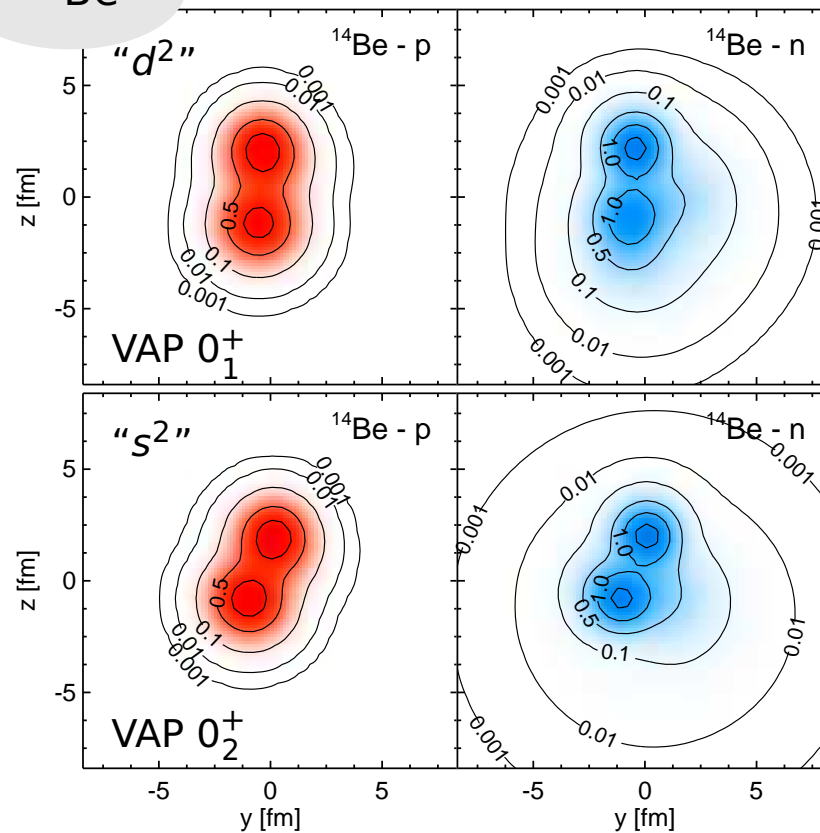
Beryllium Isotopes

Variation after Projection

^{12}Be

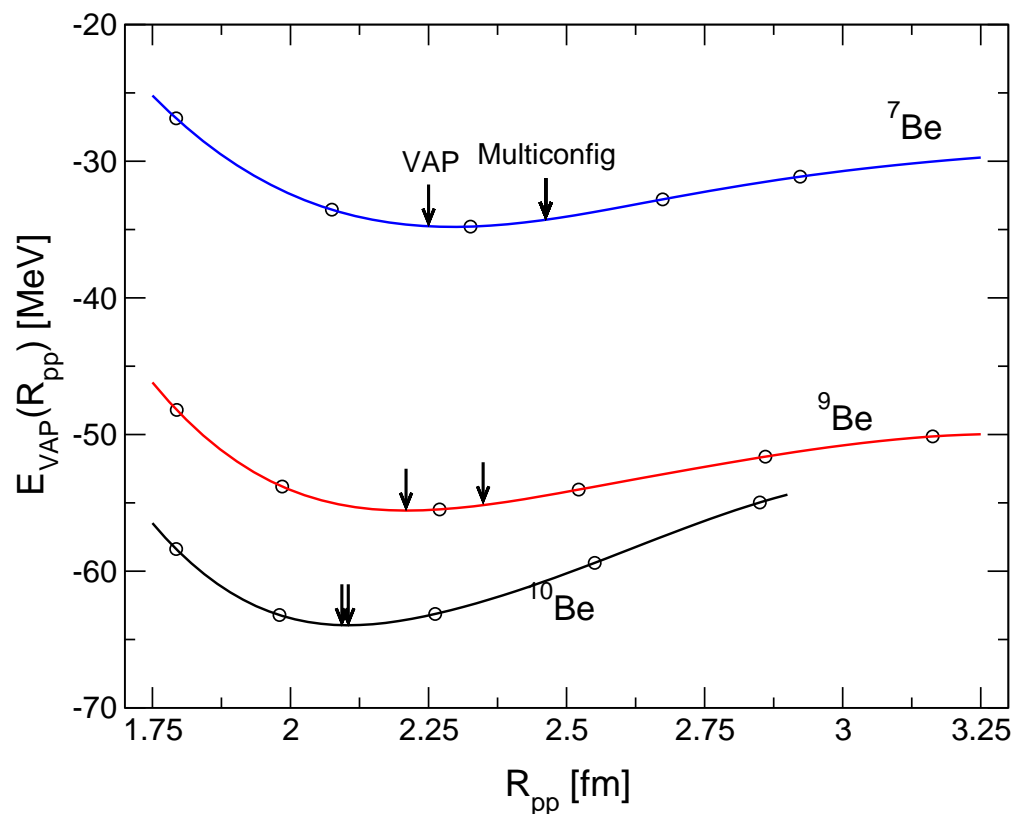


^{14}Be



Beryllium Isotopes

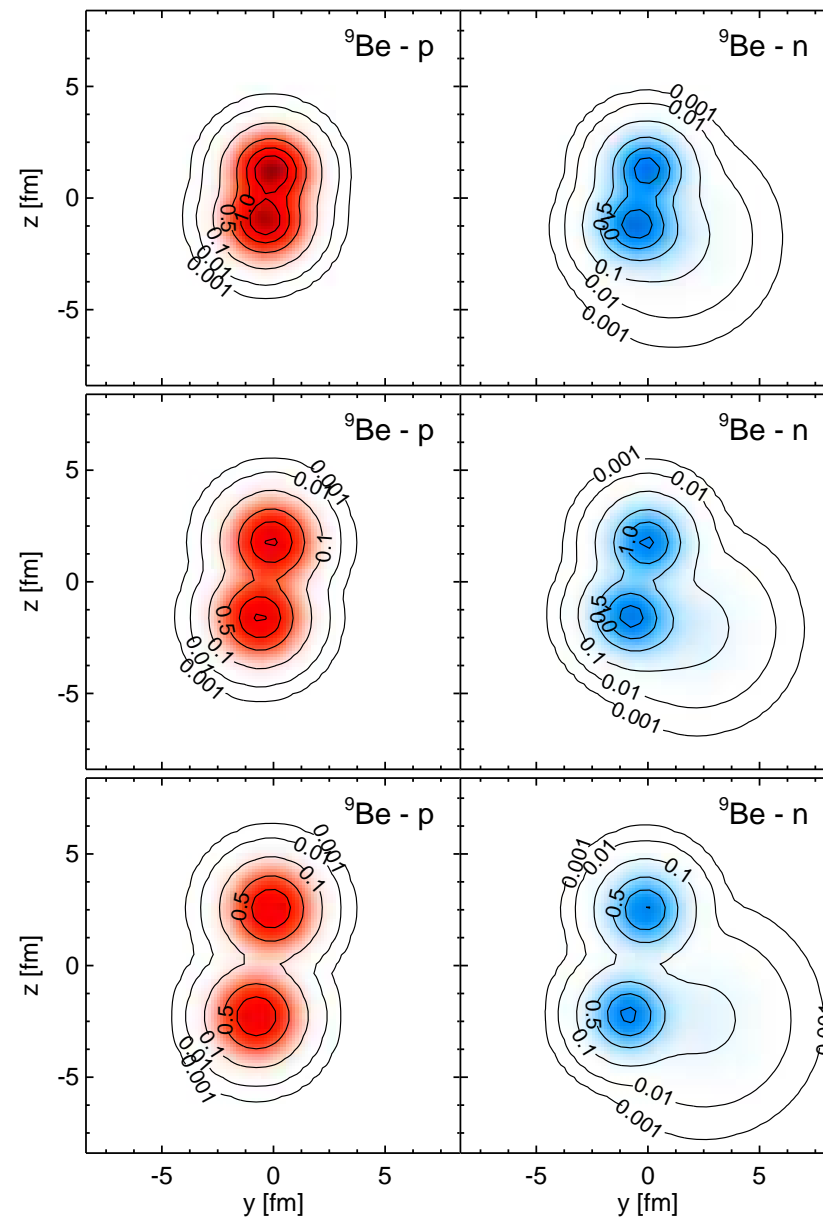
Mean proton distance as generator coordinate



Mean proton distance

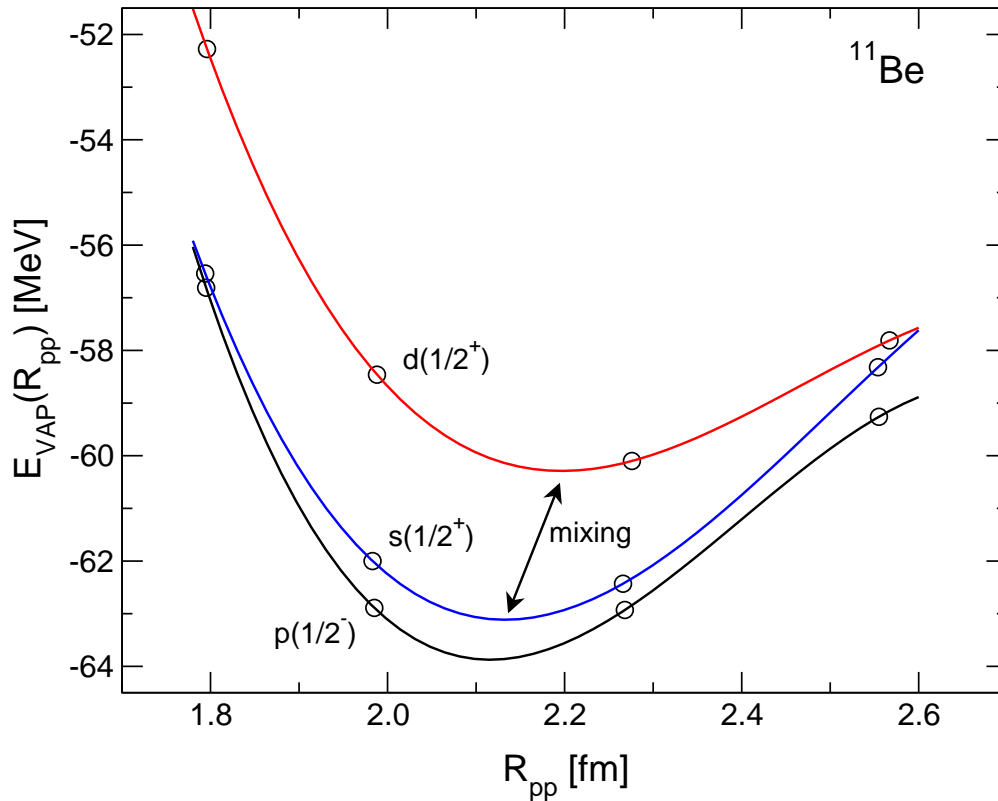
$$R_{pp}^2 = \frac{1}{Z^2} \left\langle \sum_{i < j}^{\text{protons}} (\mathbf{r}_i - \mathbf{r}_j)^2 \right\rangle$$

R_{pp} as a measure of α -cluster distance



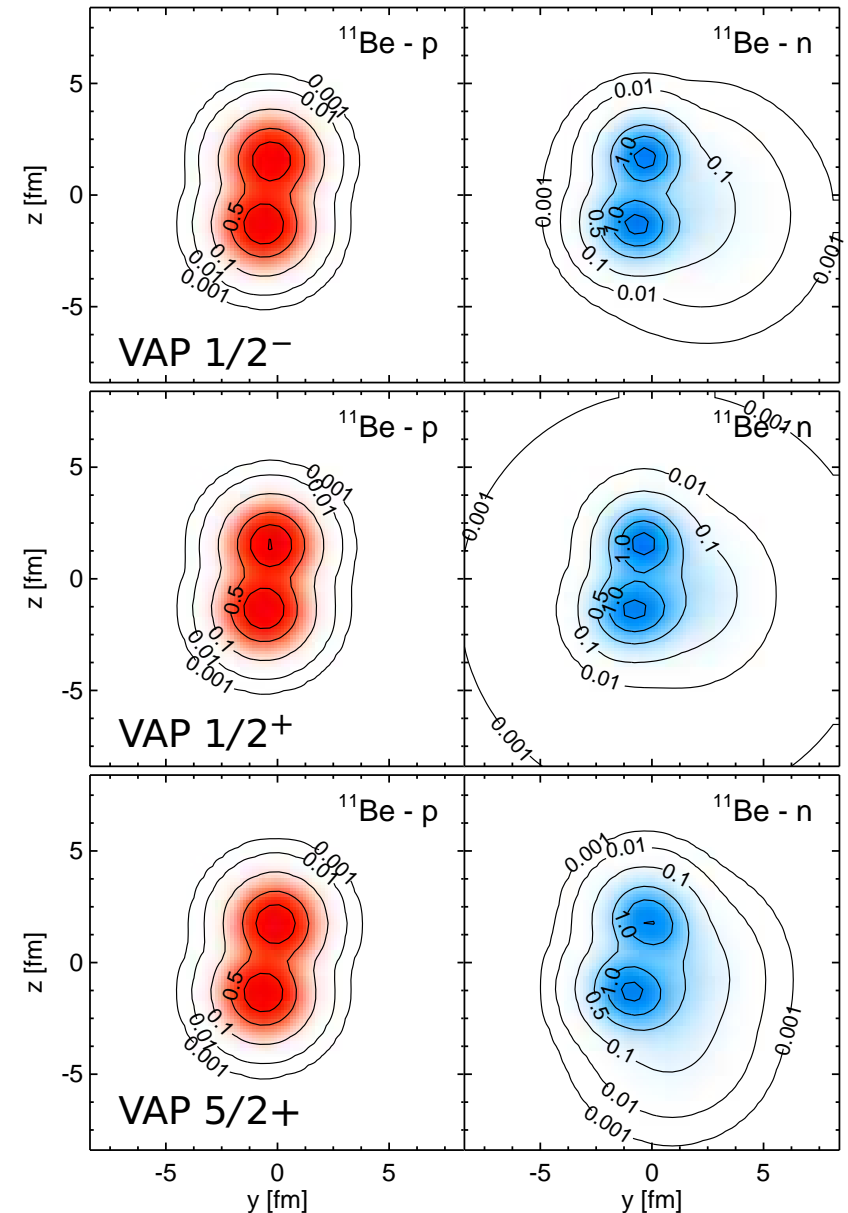
Beryllium Isotopes

Mean proton distance as generator coordinate



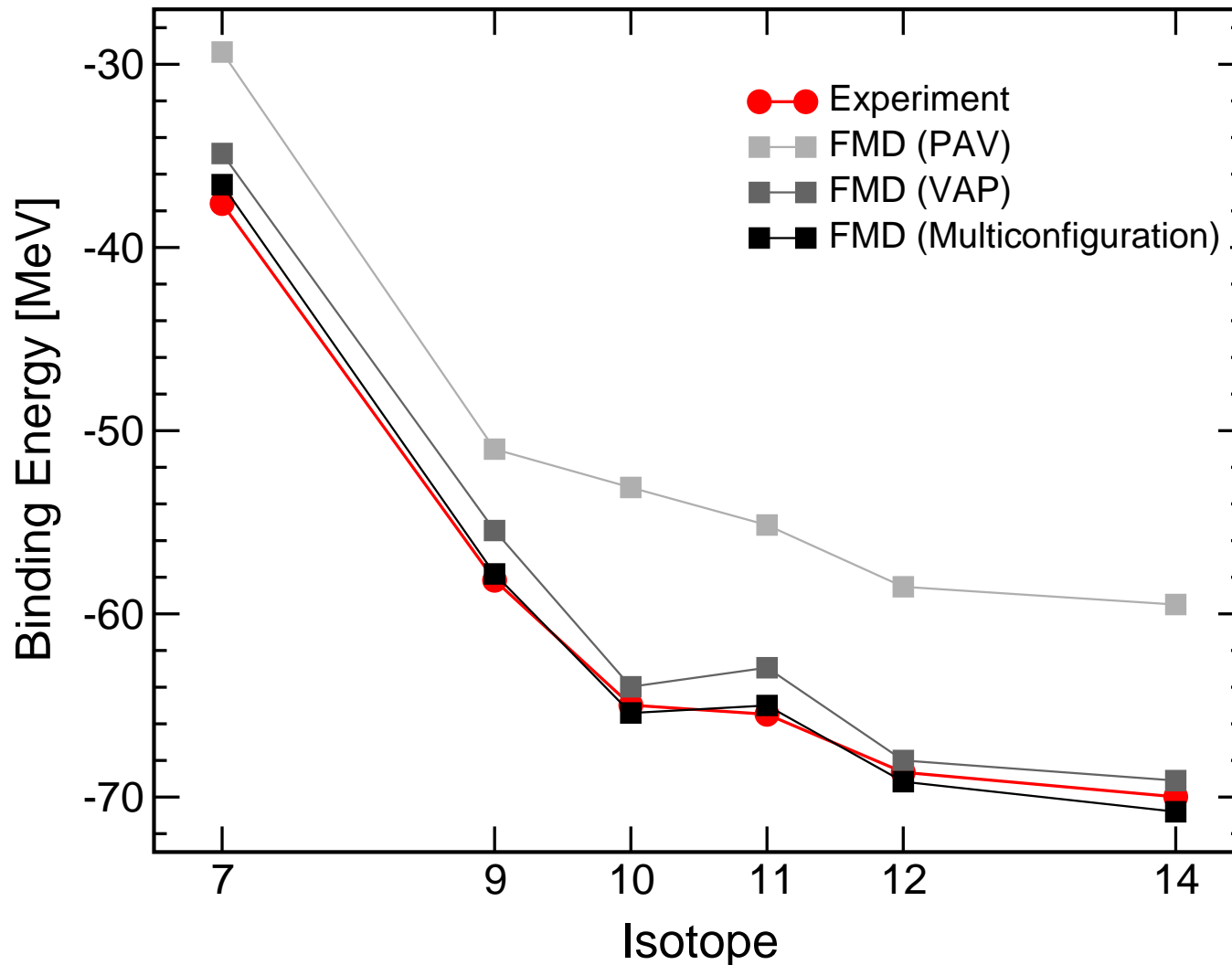
^{11}Be - "p", "s" and "d"-configurations

- "s"- and "d"-configurations will mix in $1/2^+$ state
- energy surfaces for "p" and "s" similar to those in ^{10}Be
- "d" surface has minimum at larger cluster distance \rightarrow d-configuration has a polarized ^{10}Be core



Beryllium Isotopes

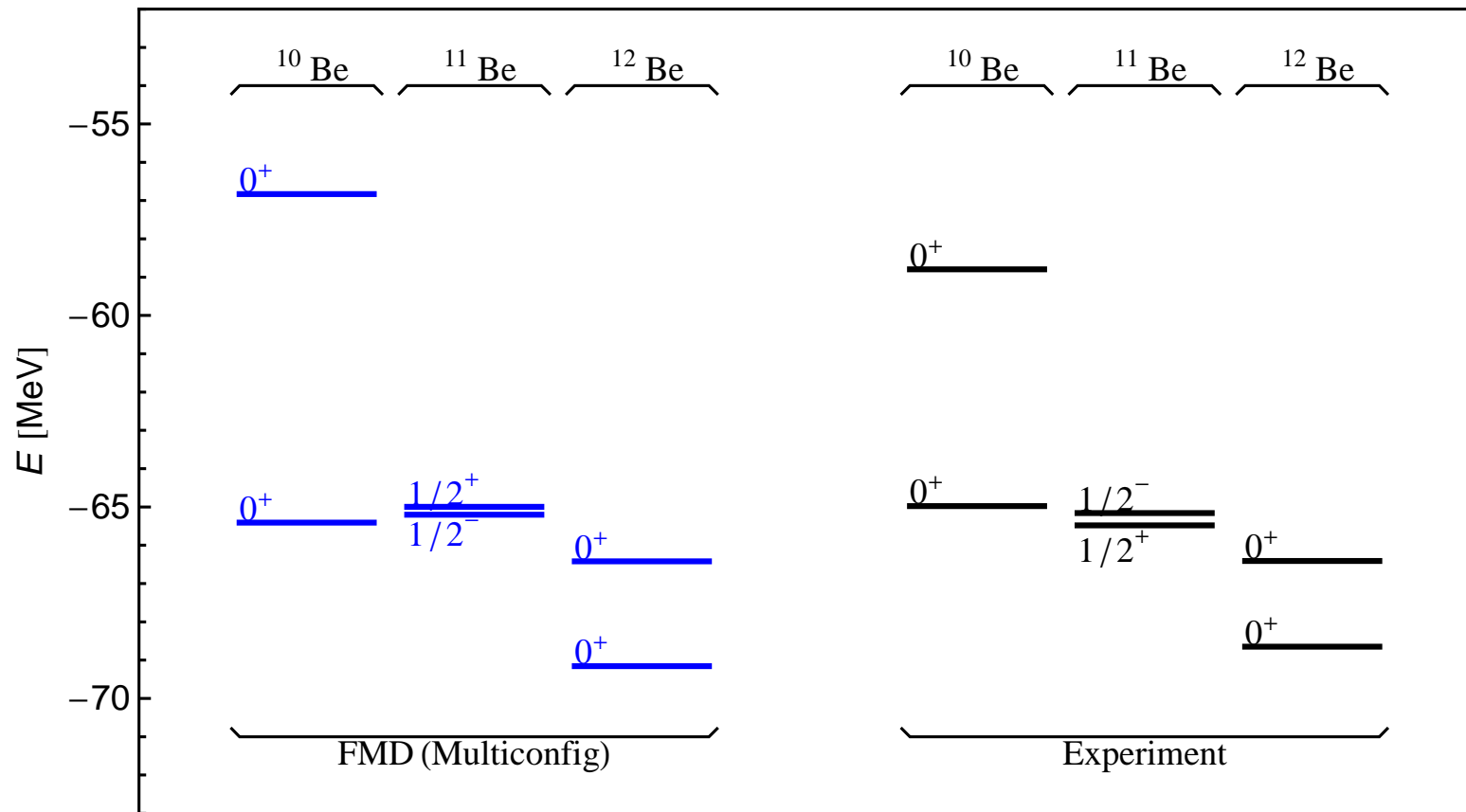
Binding energies



- large correlation energies due to cluster structure
- loosely bound systems gain most by configuration mixing

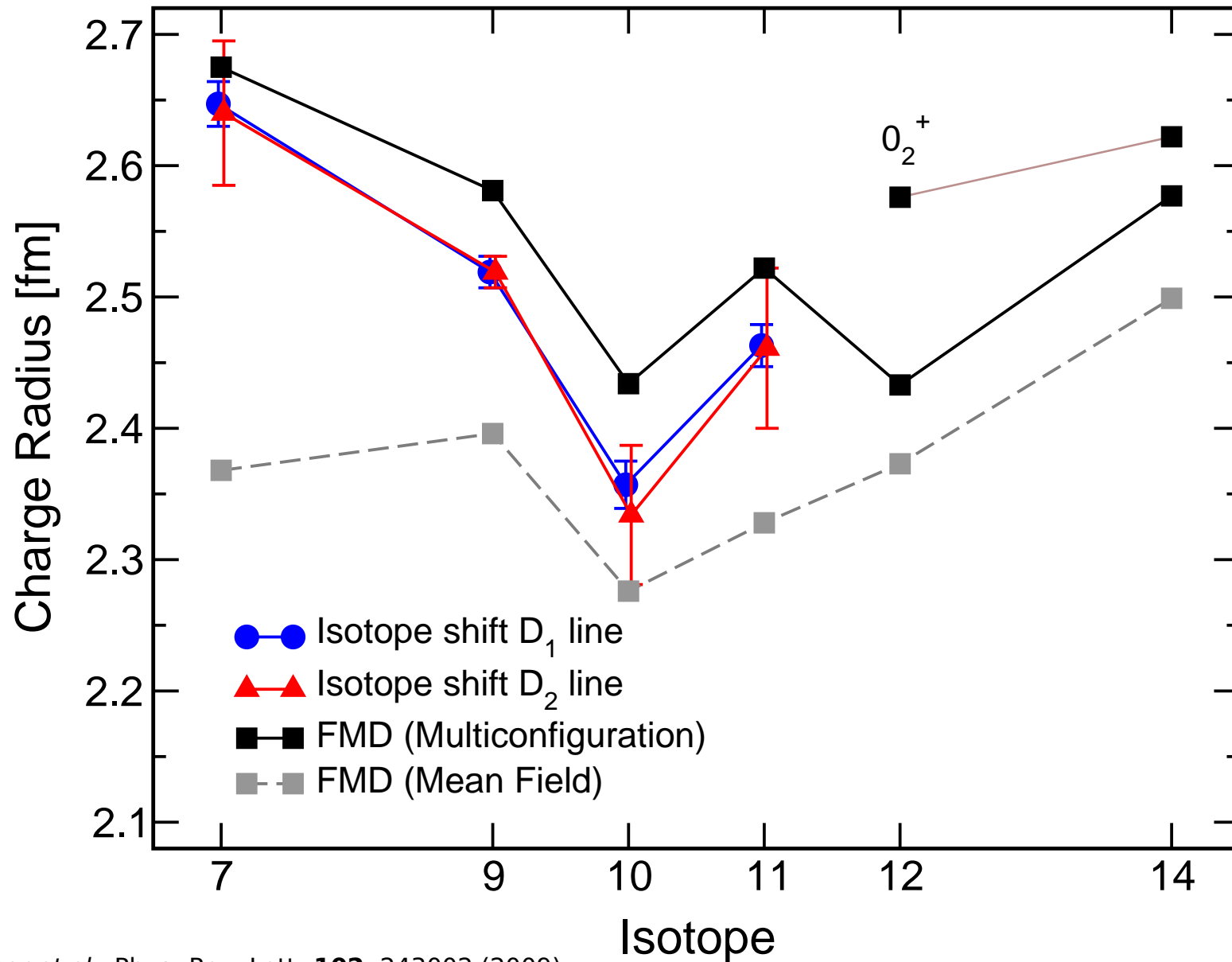
Beryllium Isotopes

$N = 8$ Shell Closure ?



- "almost correct" level ordering in ^{11}Be
- ^{12}Be ground state dominated by p^2 configuration, sizeable admixture of s^2 and d^2 configurations which strongly mix

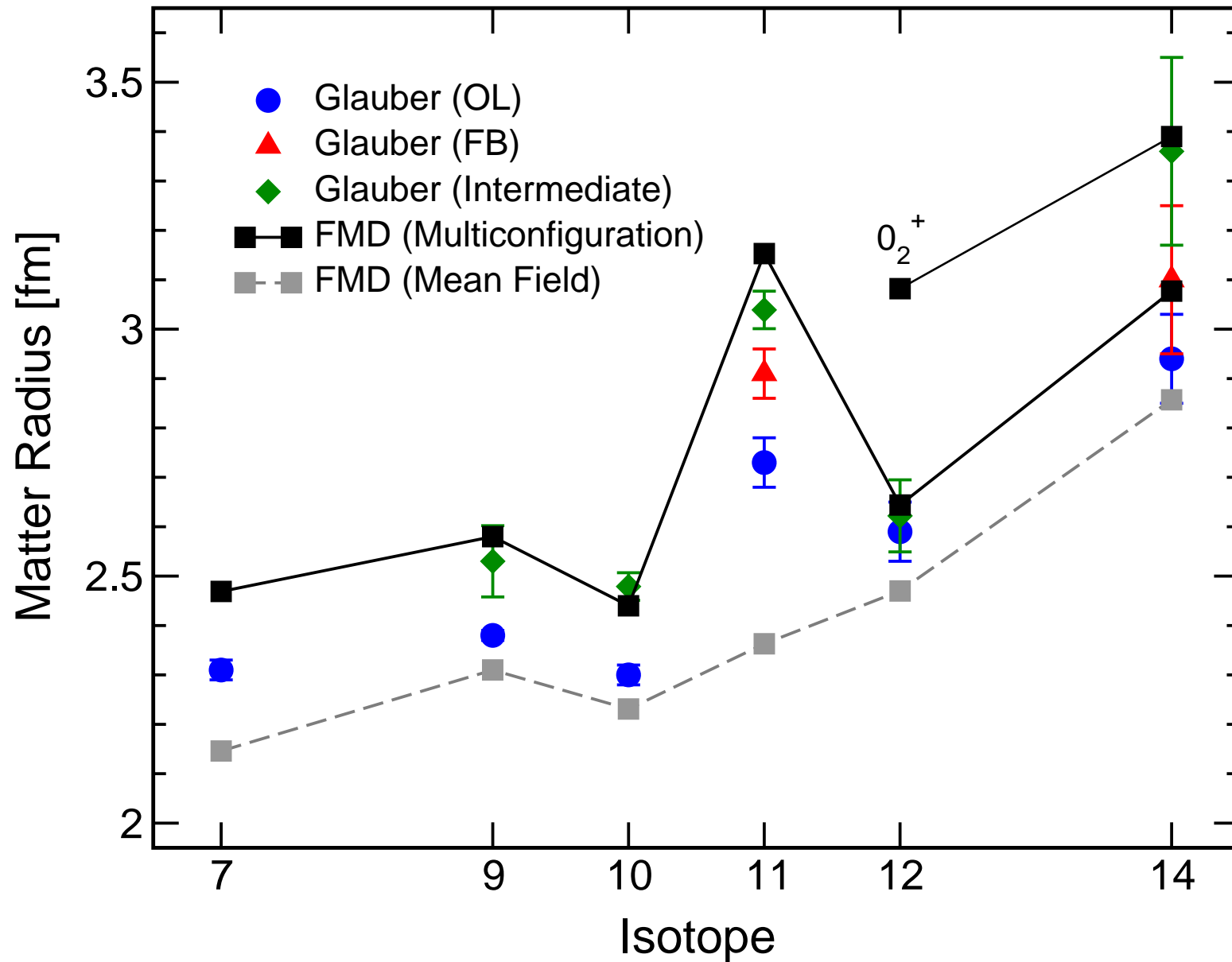
Beryllium Isotopes Charge Radii



Nörtershäuser *et al.*, Phys. Rev. Lett. **102**, 243002 (2009)

Zakova, Neff, *et al.*, J. Phys. G **37**, 055107 (2010)

Beryllium Isotopes Matter Radii



Beryllium Isotopes

Electromagnetic transitions

^{10}Be

	FMD(Multiconfig)	Experiment
$B(E2; 2_1^+ \rightarrow 0_1^+)$	$11.27 e^2\text{fm}^4$	$9.2 \pm 0.3 e^2\text{fm}^4$
$B(E2; 2_2^+ \rightarrow 0_1^+)$	$1.00 e^2\text{fm}^4$	$0.11 \pm 0.02 e^2\text{fm}^4$
$B(E2; 0_2^+ \rightarrow 2_1^+)$	$4.99 e^2\text{fm}^4$	$3.2 \pm 1.9 e^2\text{fm}^4$
$B(E1; 0_2^+ \rightarrow 1_1^-)$	$0.013 e^2\text{fm}^2$	$0.013 \pm 0.004 e^2\text{fm}^2$

^{11}Be

	FMD(Multiconfig)	Experiment
$B(E1; 1/2_1^+ \rightarrow 1/2_1^-)$	$0.020 e^2\text{fm}^2$	$0.099 \pm 0.010 e^2\text{fm}^2$

^{12}Be

	FMD(Multiconfig)	Experiment
$B(E2; 2_1^+ \rightarrow 0_1^+)$	$8.27 e^2\text{fm}^4$	$8.0 \pm 3.0 e^2\text{fm}^4$
$B(E2; 0_2^+ \rightarrow 2_1^+)$	$6.50 e^2\text{fm}^4$	$7.0 \pm 0.6 e^2\text{fm}^4$
$M(E0; 0_1^+ \rightarrow 0_2^+)$	$1.05 e\text{fm}^2$	$0.87 \pm 0.03 e\text{fm}^2$
$B(E1; 0_1^+ \rightarrow 1_1^-)$	$0.08 e^2\text{fm}^2$	$0.051 \pm 0.003 e^2\text{fm}^2$

McCutchan *et al.*, Phys. Rev. Lett. **103**, 192501 (2009).

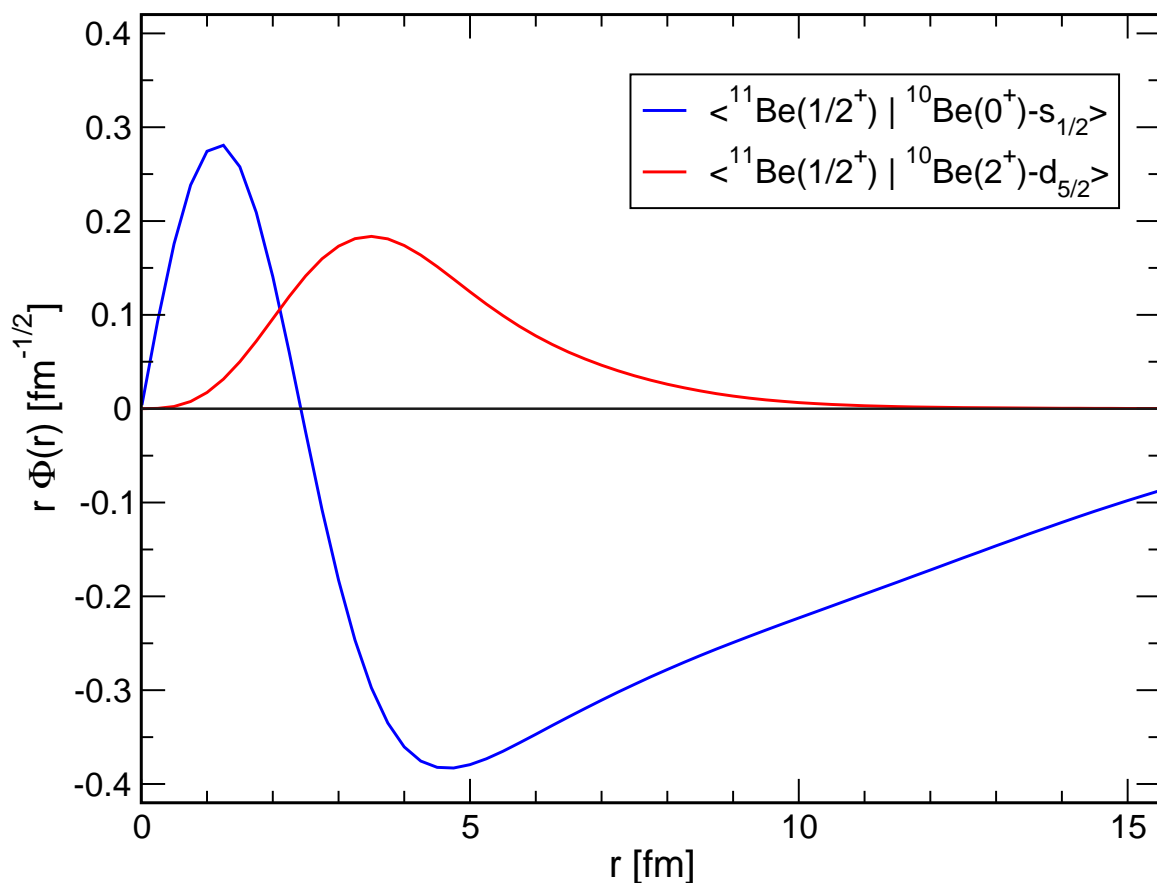
Nakamura *et al.*, Phys. Lett. **B394**, 11 (1997).

Shimoura *et al.*, Phys. Lett. **B654**, 87 (2007).

Iwasaki *et al.*, Phys. Lett. **B491**, 8 (2000).

Imai *et al.*, Phys. Lett. **B673**, 179 (2009).

^{11}Be - ^{10}Be Overlaps



Spectroscopic Factors

^{11}Be	^{10}Be	l_j	S
$1/2^+$	0^+	$s_{1/2}$	0.937
	2^+	$d_{5/2}$	0.094
	2^+	$d_{3/2}$	0.007
$5/2^+$	0^+	$d_{5/2}$	0.543
	2^+	$s_{1/2}$	0.329
	2^+	$d_{5/2}$	0.243
$1/2^-$	0^+	$p_{1/2}$	0.805
	2^+	$p_{3/2}$	0.779

- extended s-wave halo
- $s_{1/2}$ spectroscopic factor larger than results obtained from knockout and transfer reactions

Summary

Unitary Correlation Operator Method

- Explicit description of short-range central and tensor correlations
- Decouples low- and high-momentum modes

Fermionic Molecular Dynamics

- Microscopic many-body approach using Gaussian wave-packets
- Projection and multiconfiguration mixing
- Consistent description of well bound states with shell structure and loosely bound states of cluster or halo nature

Beryllium Isotopes

- α -clustering, disappearance of $N = 8$ shell closure
- s-wave halo in ^{11}Be , spectroscopic amplitudes
- ^{12}Be ground state dominantly p^2 – consistent with matter radius, waiting for charge radius measurement
- charge and matter radii, electromagnetic transitions

Thanks



to my Collaborators

**S. Bacca, A. Cribeiro, R. Cussons, H. Feldmeier, P. J. Ginsel,
B. Hellwig, K. Langanke, R. Torabi, D. Weber**

GSI Darmstadt

H. Hergert, R. Roth

Institut für Kernphysik, TU Darmstadt